



Technical Report
RAL-TR-96-062

A Possible Explanation of the " $\rho\pi$ Puzzle" in J/Ψ , Ψ' Decays

X-Q Li

August 1996

© Council for the Central Laboratory of the Research Councils 1996

Enquiries about copyright, reproduction and requests for additional copies of this report should be addressed to:

The Central Laboratory of the Research Councils

Library and Information Services

Rutherford Appleton Laboratory

Chilton

Didcot

Oxfordshire

OX11 0QX

Tel: 01235 445384 Fax: 01235 446403

E-mail library@rl.ac.uk

ISSN 1358-6254

Neither the Council nor the Laboratory accept any responsibility for loss or damage arising from the use of information contained in any of their reports or in any communication about their tests or investigations.

A Possible Explanation of the “ $\rho\pi$ Puzzle” in J/Ψ , Ψ' Decays

Xue-Qian Li

Rutherford Appleton Laboratory,
Chilton, Didcot, OX11 0QX, UK

and

Department of Physics, Nankai University
Tianjin 300071, China

David V. Bugg and Bing-Song Zou

Queen Mary and Westfield College,
London E1 4NS, UK

Abstract

We evaluate the contributions of final state interactions (FSI) to $J/\Psi \rightarrow \rho\pi$ and $\Psi' \rightarrow \rho\pi$ with various intermediate physical channels. We find that the rescattering of $a_2\rho$ and $a_1\rho$ into $\rho\pi$ can change the $\rho\pi$ production rate substantially, and therefore could be an explanation for the longstanding “ $\rho\pi$ puzzle”. The FSI effects may also play a significant role for other channels, such as $K^*\bar{K}$ and $f_2\omega$.

PACS number(s): 13.75.Lb, 13.20.Gd, 13.25, 14.40

I. Introduction

The mysterious $\Psi' \rightarrow \rho\pi$ suppression puzzle has lingered for a long while, but remains unanswered [1, 2]. According to perturbative QCD, for any specific final hadronic state h , one expects

$$Q_h \equiv \frac{B(\Psi' \rightarrow h)}{B(J/\Psi \rightarrow h)} \approx \frac{B(\Psi' \rightarrow e^+e^-)}{B(J\Psi \rightarrow e^+e^-)} = 0.147 \pm 0.023[3]. \quad (1)$$

While this is true for many hadronic states[3], it fails for $\rho\pi$ and K^*K final states [1, 2]; the present experimental limits[2] for $\rho\pi$ and $K^*\bar{K}$ final states are one to two orders of magnitude smaller:

$$Q_{\rho\pi} < 0.0028 \quad \text{and} \quad Q_{K^*K} < 0.011. \quad (2)$$

Brodsky, Lepage and Tuan [4] proposed that there might be a gluonium intermediate state with a mass very close to $M_{(J/\Psi)}$, so that the resonance effect greatly enhances the rate of $J/\Psi \rightarrow \rho\pi$ compared to $\Psi' \rightarrow \rho\pi$. However, the recent data of BEPC seem not to support the existence of glueballs within this mass range[2], so one has to search for other explanations of the $\Psi' \rightarrow \rho\pi$ suppression.

Generally, before claiming probable new physics applying to a process which seems exotic, one should try all well-known mechanisms and see if the mystery can be interpreted in the existing theoretical framework. Motivated by this idea, we try to analyze the contributions of the final state interactions (FSI) to the $\Psi' \rightarrow \rho\pi$ suppression.

The FSI plays a very important, sometimes crucial role in many exclusive processes. Isgur et al.[5] considered the $\pi\pi$ FSI to explain the $\Delta I = \frac{1}{2}$ rule in $K \rightarrow \pi\pi$ decays. Lipkin et al.[6] suggested that hadronic loops may result in OZI-rule violation for $(u\bar{u} + d\bar{d})$ - $s\bar{s}$ mixing and some ϕ production rates. Anisovich et al.[7] studied FSI effects in many three-body decay channels. Locher et al.[8] established a practical way to evaluate the contribution of hadronic loops to ϕ and f'_2 productions from $p\bar{p}$ annihilation. It turns out that the FSI gives rise to substantial contributions. The method for evaluation of hadronic loops is proved to be reliable and appropriate to practical calculations. Such calculations depend on and are well constrained by the

input experimental data. There may be a factor of 2~3 uncertainty for the results. However the physical picture is usually determined by the order of magnitude.

With this understanding in mind, it is natural to apply this method to calculate the hadronic loop contributions to the interesting final states from J/Ψ and Ψ' decays. Here we calculate the contributions from loop diagrams shown in Fig.1. Fig.1a is unique to $\Psi' \rightarrow \rho\pi$. Here σ stands for the low energy $\pi\pi$ S-wave amplitude[9]. If this contribution is large, it could give a natural explanation for the difference of $\rho\pi$ production rates from J/Ψ and Ψ' . Unfortunately, we find its contribution to be negligible compared to the experimental value, due to the exchanged pion being too far off-shell for the on-shell J/Ψ and σ intermediate state. The reason for considering Fig.1b is the following. The largest hadronic decay channel observed for J/Ψ decays is $2(\pi^+\pi^-)\pi^0$, where its largest contributions come from intermediate $a_2\rho$ states [3] and possibly also from $a_1\rho$ states which may not have been identified due to the large width of the a_1 . Both $a_2(1320)$ and $a_1(1230)$ have $\rho\pi$ as their dominant decay mode, and can rescatter into $\rho\pi$ by exchanging the lightest meson, the pion; they may therefore make substantial contributions to the $\rho\pi$ final states. Our results confirm this expectation. Their contributions to $\rho\pi$ have the same order of magnitude as the experimentally observed $\rho\pi$ rate. The relative phases between loop diagrams and the tree diagram cannot be determined at the present stage. Thus we are only able to conclude that it is a possibility that the interference effect between these diagrams may cause the difference of the $\rho\pi$ rates from J/Ψ and Ψ' .

In the next section, we describe the method and the formulation for evaluating the dominant hadronic loops for $J/\Psi \rightarrow \rho\pi$ as shown in Fig.1b. In Sec.III, we give the numerical results and discussions.

II. The method and the formulation

Following the formalism of [8], the amplitude T corresponding to the diagram in Fig.1b is

$$T = \frac{i}{(2\pi)^4} \int d^4 k_a \frac{T_{\Psi a\rho} T_{a\rho\pi} T_{\rho\pi\pi}}{(k_a^2 - m_a^2 + i\epsilon)(k_\rho^2 - m_\rho^2 + i\epsilon)(k_\pi^2 - m_\pi^2 + i\epsilon)}. \quad (3)$$

Here the amplitudes $T_{\Psi a\rho}$, $T_{a\rho\pi}$ and $T_{\rho\pi\pi}$ are for the $\Psi a\rho$, $a\rho\pi$ and $\rho\pi\pi$ three-body

vertices, respectively, with Ψ taken to be J/Ψ or Ψ' and a to be $a_2(1320)$ or $a_1(1230)$. Also k_a , k_ρ and k_π are 4-momenta of the a , ρ and π , respectively, on the loop.

By the Cutkosky rule, the amplitude (3) for the on-shell $a\rho$ intermediate state can be easily reduced to the solid angle integration as

$$T_{\Psi \rightarrow a\rho \rightarrow \rho\pi}^{on-shell} = \frac{-iK_a}{32\pi^2 M_\Psi} \int d\Omega \frac{T_{\Psi a\rho} T_{a\rho\pi} T_{\rho\pi\pi}}{m_a^2 + m_\rho^2 - m_\pi^2 - 2E_a E_\rho + 2K_a P_\rho \cos\theta}, \quad (4)$$

where K_a and P_ρ are the magnitudes of the 3-momenta of the on-shell a and the ρ in the final state, respectively; E_a and E_ρ are corresponding energies. The amplitude (4) is usually called the unitarity approximation.

We define the effective vertices in the relativistic notation [8, 10] as follows:

- The amplitude for $\Psi \rightarrow a_2\rho$ with the smallest number of derivatives is

$$T_{\Psi a_2\rho} = g_{\Psi a_2\rho} e^\mu(\Psi, m_1) \phi_{\mu\nu} e^\nu(\rho, m_2), \quad (5)$$

where $\phi_{\mu\nu}$ is the polarization tensor of a_2 ; $e^\mu(\Psi, m_1)$ and $e^\nu(\rho, m_2)$ are the polarization vectors of Ψ and ρ , respectively. The coupling constant $g_{\Psi a_2\rho}$ is related to the $J/\Psi \rightarrow a_2\rho$ rate by

$$\Gamma_{J/\Psi \rightarrow a_2\rho} = \frac{5K_{a_2}g_{\Psi a_2\rho}^2}{24\pi M_\Psi^2} \left\{ 1 + \frac{K_{a_2}^2}{3m_{a_2}^2} \left(1 + \frac{M_\Psi^2}{m_\rho^2} \right) + \frac{2M_\Psi^2 K_{a_2}^4}{15m_\rho^2 m_{a_2}^4} \right\}, \quad (6)$$

which gives $g_{\Psi a_2\rho} = 4.4 \times 10^{-3} GeV$.

- The amplitude for $J/\Psi \rightarrow a_1\rho$ with the smallest number of derivatives is

$$T_{\Psi a_1\rho} = g_{\Psi a_1\rho} \epsilon_{\mu\nu\alpha\beta} p_\Psi^\mu e^\nu(\Psi, m_1) e^\alpha(a_1, m_3) e^\beta(\rho, m_2). \quad (7)$$

The coupling constant $g_{\Psi a_1\rho}$ is related to the $J/\Psi \rightarrow a_1\rho$ rate by

$$\Gamma_{J/\Psi \rightarrow a_1\rho} = \frac{K_{a_1}g_{\Psi a_1\rho}^2}{4\pi} \left(1 + \frac{K_{a_1}^2}{3m_{a_1}^2} + \frac{K_{a_1}^2}{3m_\rho^2} \right), \quad (8)$$

which gives $g_{\Psi a_1\rho} = 2.2 \times 10^{-3}$ if we make the guess that $\Gamma_{J/\Psi \rightarrow a_1\rho} = \Gamma_{J/\Psi \rightarrow a_2\rho}$.

- The amplitude for $\Psi \rightarrow \rho\pi$ is

$$T_{\Psi\rho\pi} = g_{\Psi\rho\pi} \epsilon_{\mu\nu\alpha\beta} p_\Psi^\mu e^\nu(\Psi, m_1) p_\rho^\alpha e^\beta(\rho, m_2). \quad (9)$$

The coupling constant $g_{\Psi\rho\pi}$ is related to the $J/\Psi \rightarrow \rho\pi$ rate by

$$\Gamma_{J/\Psi \rightarrow \rho\pi} = \frac{1}{12\pi} g_{\Psi\rho\pi}^2 P_\rho^3, \quad (10)$$

which gives $g_{\Psi\rho\pi} = 3.74 \times 10^{-3}/GeV$.

- The amplitude for $a_2 \rightarrow \rho\pi$ is

$$T_{a_2\rho\pi} = g_{a_2\rho\pi} \epsilon_{\mu\nu\alpha\beta} k_{a_2}^\mu e^\nu(\rho, m_2) p_\rho^\alpha \phi^{\beta\beta'}(p_\rho)_{\beta'}. \quad (11)$$

The coupling constant $g_{a_2\rho\pi}$ is related to the $a_2 \rightarrow \rho\pi$ rate by

$$\Gamma_{a_2 \rightarrow \rho\pi} = \frac{1}{40\pi} g_{a_2\rho\pi}^2 P_\rho^5, \quad (12)$$

which gives $g_{a_2\rho\pi} = 1.69 GeV^{-2}$.

- The amplitude for $a_1 \rightarrow \rho\pi$ with the smallest number of derivatives is

$$T_{a_1\rho\pi} = g_{a_1\rho\pi} e^\mu(a_1, m_3) e_\mu(\rho, m_2) \quad (13)$$

with $g_{a_1\rho\pi} = 6.54 GeV$.

- The amplitude for $\rho \rightarrow \pi\pi$ is

$$T_{\rho\pi\pi} = g_{\rho\pi\pi} e_\mu(\rho, m_2) \cdot (p_\pi^\mu - k_\pi^\mu) \quad (14)$$

where p_π and k_π are 4-momenta for the two pions of the ρ decay, $g_{\rho\pi\pi} = 6.05$.

In principle, some more complicated Lorentz forms including more derivatives are also allowed for $\Psi \rightarrow a_{2,1}\rho$ and $a_1 \rightarrow \rho\pi$, and could be considered. However, to serve the purpose of this work, only the order of magnitude is required, so the lowest order Lagrangian is sufficient. In this paper we also limit ourselves to the unitarity approximation of amplitude (4). The full amplitude can be calculated using a dispersive relation with some additional cut-off parameters; its magnitude

will necessarily be larger than that of the unitarity approximation but will not change the order of magnitude[8].

In the unitarity approximation, only the exchanged pion is off-shell. To account correctly for the off-shell effects of the pion, we have to include in the integration of Eq.(4) an additional off-shell form factor

$$\left(\frac{\Lambda^2 - m_\pi^2}{\Lambda^2 - k_\pi^2}\right)^2 = \left(\frac{\Lambda^2 - m_\pi^2}{\Lambda^2 - m_a^2 - m_\rho^2 + 2E_a E_\rho - 2K_a P_\rho \cos\theta}\right)^2 \quad (15)$$

where Λ is a scale parameter with a reasonable range of $1.2 \sim 2.0$ GeV[8]. The resulting decay width of $\Psi \rightarrow \rho\pi$ is

$$\Gamma_{\Psi \rightarrow a\rho \rightarrow \rho\pi} = \frac{P_\rho}{8\pi M_\Psi^2} \frac{1}{3} \sum_{m_1, m_2} |T_{\Psi \rightarrow a\rho \rightarrow \rho\pi}^{on-shell}|^2. \quad (16)$$

From the above equations and following the helicity-coupling amplitude method which is described in every detail by Chung[10], the entire calculations are straightforward but very tedious. The numerical results are given in the following section.

III. Numerical results and discussions

Assuming the unitarity approximation with $\Lambda = 1.6$ GeV, we obtain

$$\Gamma_{J/\Psi \rightarrow a_2 \rho \rightarrow \rho\pi}^{on-shell} = 0.69 \text{ keV}, \quad (17)$$

$$\Gamma_{J/\Psi \rightarrow a_1 \rho \rightarrow \rho\pi}^{on-shell} = 0.031 \frac{\Gamma_{J/\Psi \rightarrow a_1 \rho}}{\Gamma_{J/\Psi \rightarrow a_2 \rho}} \text{ keV}. \quad (18)$$

Changing Λ in the range of $1.2 \sim 2.0$ GeV, the above results will change by a factor of less than 2. The on-shell approximation only includes the imaginary part of the amplitudes; by including the real part of the amplitudes, we can get even larger values. We see that the a_2 loop diagram, Eq.(17), can give a contribution of the same order of magnitude as the experimental data, $\Gamma_{J/\Psi \rightarrow \rho\pi} = (1.1 \pm 0.1)$ keV, and may play a dominant role. The rate for $J/\Psi \rightarrow a_1 \rho$ is not known experimentally, hence we cannot evaluate the magnitude of the a_1 loop diagram. However, if $\Gamma_{J/\Psi \rightarrow a_1 \rho}$ is of the same order of magnitude as $\Gamma_{J/\Psi \rightarrow a_2 \rho}$, Eq.(18) shows that the $a_1 \rho$ loop diagram would be smaller than that for $a_2 \rho$.

Secondly, using the same formulae for J/Ψ and Ψ' we find

$$\frac{B_{\Psi' \rightarrow a_2 \rho \rightarrow \rho\pi}^{\text{on-shell}}}{B_{J/\Psi \rightarrow a_2 \rho \rightarrow \rho\pi}^{\text{on-shell}}} \approx 0.22 \frac{B_{\Psi' \rightarrow a_2 \rho}^{\text{tree}}}{B_{J/\Psi \rightarrow a_2 \rho}^{\text{tree}}}, \quad (19)$$

$$\frac{B_{\Psi' \rightarrow a_1 \rho \rightarrow \rho\pi}^{\text{on-shell}}}{B_{J/\Psi \rightarrow a_1 \rho \rightarrow \rho\pi}^{\text{on-shell}}} \approx 1.21 \frac{B_{\Psi' \rightarrow a_1 \rho}^{\text{tree}}}{B_{J/\Psi \rightarrow a_1 \rho}^{\text{tree}}}. \quad (20)$$

The difference in the numerical factors in these relations arises from the different vertices and loop kinematics for the $a_2\rho$ loop and the $a_1\rho$ loop. Relative to the direct tree-production of $a_2\rho$ and $a_1\rho$, Eq.(19) shows that the contribution from the $a_2\rho$ loop to $\rho\pi$ is much smaller for Ψ' than for J/Ψ ; in contrast, Eq.(20) says that the contribution from the $a_1\rho$ loop to $\rho\pi$ is slightly stronger for Ψ' than for J/Ψ .

Thirdly, preliminary results[11] from the BES collaboration at BEPC give

$$\frac{B(\Psi' \rightarrow a_2 \rho)}{B(J/\Psi \rightarrow a_2 \rho)} = 0.044 \pm 0.032. \quad (21)$$

This is smaller than the prediction of Eq.(1). If we assume that the direct tree-production rates for $a_2\rho$ and $a_1\rho$ have approximately the same value, then from Eq.(19) we have

$$\frac{B_{\Psi' \rightarrow a_2 \rho \rightarrow \rho\pi}^{\text{on-shell}}}{B_{J/\Psi \rightarrow a_2 \rho \rightarrow \rho\pi}^{\text{on-shell}}} \approx 0.0097. \quad (22)$$

This rate is much smaller than the value of Eq.(1), but not so small as the ratio $Q_{\rho\pi}$ given by Eq.(2).

Some special mechanism is required to explain the very low rate of $\Psi' \rightarrow \rho\pi$. We envisage the possibility of a cancellation between the $a_2\rho$ loop diagram, the $a_1\rho$ loop diagram and the tree diagram. The same cancellation is unlikely to occur for $J/\Psi \rightarrow \rho\pi$: if we use Eq.(22) for the $a_2\rho$ loop and Eqs.(20) and (1) for the $a_1\rho$ loop, the ratio of $a_2\rho$ loop to the $a_1\rho$ loop is likely to be a factor of 10 or more larger for J/Ψ than for Ψ' . It suggests that the $a_2\rho$ loop diagram may be large enough to dominate $J/\Psi \rightarrow \rho\pi$.

Of course the real physics situation may be more complicated. The coupling constants given in Sect.II are only true for the tree level where the FSI is neglected. The true values will deviate from these values because of FSI effects. In principle,

we should fit them from equations

$$\begin{aligned} T(\Psi \rightarrow \rho\pi) &= T_{tree}(\Psi \rightarrow \rho\pi) + T(\Psi \rightarrow a_1\rho \rightarrow \rho\pi) + T(\Psi \rightarrow a_2\rho \rightarrow \rho\pi) \\ T(\Psi \rightarrow a_1\rho) &= T_{tree}(\Psi \rightarrow a_1\rho) + T(\Psi \rightarrow \rho\pi \rightarrow a_1\rho) + T(\Psi \rightarrow a_2\rho \rightarrow a_1\rho) \\ T(\Psi \rightarrow a_2\rho) &= T_{tree}(\Psi \rightarrow a_2\rho) + T(\Psi \rightarrow \rho\pi \rightarrow a_2\rho) + T(\Psi \rightarrow a_1\rho \rightarrow a_2\rho), \end{aligned} \quad (23)$$

where we have only taken into account the channels which possess the larger branching ratios. We should also consider higher loop contributions since they are large compared to the Born term. But this is almost impossible at the present stage due to technical difficulties.

The main object of this paper is to point out that the FSI in J/Ψ and Ψ' decays gives rise to effects which are of the same order as the tree level amplitudes, and may be a possible explanation for the long-standing $\rho\pi$ puzzle. Our explanation is that $J/\Psi \rightarrow \rho\pi$ is strongly enhanced by the $a_2\rho$ loop diagram. The direct tree-production for $\rho\pi$ may be suppressed by the hadronic helicity conservation mechanism[12]. The contribution of the $a_1\rho$ loop diagram is much smaller than that of the $a_2\rho$ loop for the $J/\Psi \rightarrow \rho\pi$; but they have similar strength for the $\Psi' \rightarrow \rho\pi$ and may cancel each other.

The contribution of a triangle diagram will be large whenever three vertex-couplings involved are large and the exchanged meson is light as well as not too far off-shell. The similar apparent suppression for $\Psi' \rightarrow K^*\bar{K}$ and $\Psi' \rightarrow f_2\omega$ [13] may also be explained by the $K^*\bar{K}_{2,1}^*$ and $b_1\pi$ loops, respectively. Both $K^*(892)\bar{K}_2^*(1430)$ and $b_1(1235)\pi$ decay modes are observed to be very large for J/Ψ . They can rescatter into $K^*\bar{K}$ and $f_2\omega$, respectively, by exchanging a pion. Therefore the FSI may provide a coherent explanation for all observed suppressed modes of Ψ' decays. It will be very interesting for BES to check whether the $a_1\rho$ and $K_1^*\bar{K}^*$ production rates are large for Ψ' . If so, it may give further support to our mechanism.

Acknowledgments: One of us (Li) would like to thank the Rutherford Appleton Laboratory for its hospitality; the main part of the work is accomplished during the period of his visit at the lab. Zou gratefully acknowledges the support of the K.C.Wong Education Foundation, Hong Kong, for a visit to Beijing where the work was begun. We thank Chao-Hsi Chang and Guang-Da Chao for useful discussions. This work is partly supported by the National Natural Science Foundation of China.

References

- [1] M. Franklin et al. Phys.Rev.Lett. **51** (1983) 963.
- [2] BES Collaboration, J.Z.Bai et al., Phys. Rev. D **54** (1996) 1221.
- [3] Particle Data Group, L.Montanet et al., Phys.Rev. D **50** (1994) 1173.
- [4] S. Brodsky, G. Lepage and S. Tuan, Phys.Rev.lett. **59** (1987) 621.
- [5] N. Isgur, K. Maltman, I. Weinstein and T. Barnes, Phys.Rev.Lett. **64** (1990) 161; M.P.Locher, V.E.Markusin and H.Q.Zheng, Preprint PSI-PR-96-13, to be published on Phys. Rev. D.
- [6] H. Lipkin, Nucl.Phys. B244 (1984) 147; Phys.Lett. B **179** (1986) 278; Nucl.Phys. B **291** (1987) 720; H.Lipkin and B.S.Zou, Phys. Rev. D **53** (1996) 6693; P. Geiger and N. Isgur, Phys.Rev. D **47** (1993) 5050; **44** (1991) 799; Phys. Rev. Lett. **67** (1991) 1066.
- [7] V.V. Anisovich, D.V. Bugg, A.V. Sarantsev and B.S. Zou, Phys.Rev. D **51** (1995) R4619; **50** (1994) 1972.
- [8] M. Locher and Y. Lu, Z.Phys. A **351** (1994) 81; M.P.Locher, Y.Lu and B.S.Zou, Z. Phys. A **347** (1994) 281; Y. Lu, B.S. Zou and M. Locher, Z.Phys. A **345** (1993) 207; O.Gortchakov et al., Z.Phys. A **353** (1996) 447; D.Buzatu and F.M.Lev, Phys. Lett. B **329** (1994) 143; **359** (1995) 393; A.V.Anisovich and E.Klempt, Z. Phys. A **354** (1996) 197.
- [9] B.S.Zou and D.V.Bugg, Phys.Rev. D **48** (1993) R3948; **51** (1994) 591.
- [10] S.U. Chung, Phys.Rev. D **48** (1993) 1225.
- [11] J.Li, Preprint BIHEP-EP1-95-06.
- [12] S.J.Brodsky and G.P.Lepage, Phys. Rev. D **24** (1981) 2848.
- [13] Y.F.Gu and S.F.Tuan, Mod. Phys. Lett. A **10** (1995) 615.

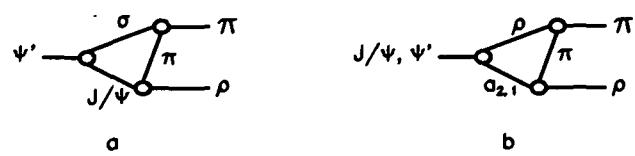


Fig.1

Figure 1: a) Triangle diagram for $\Psi' \rightarrow \Psi \sigma \rightarrow \rho \pi$ with σ standing for the $\pi\pi$ S-wave system; b) Triangle diagram for $\rho\pi$ production from J/Ψ and Ψ' through $a_2(1320)\rho$ and $a_1(1230)\rho$ intermediate states.